

A mathematical model for non-linear dynamics of conservative systems with non-homogeneous boundary conditions

V.A. Krysko, J. Awrejcewicz ^{*}, T. Molodenkova

Department of Mathematics, Saratov Technical University, 410054 Saratov, Russia

Received 4 October 2005; accepted 7 August 2006

Abstract

In this work a transition into a chaotic dynamics of plates with unmovable boundary conditions along a plate contour and subjected to a longitudinal impact action modeled as a rectangular type loading of infinite length in time is studied. The well-known T. von Kármán equations governing behaviour of flexible isotropic plates have been applied. Finite-difference approximation of order $O(h^4)$ allowed to transform the problem from PDEs to ODEs. We have shown and discussed how the investigated plate vibrations are transmitted into chaotic dynamics through a period doubling bifurcation. Furthermore, essential influence of boundary conditions on bifurcations number is illustrated, and for all investigated problems the Feigenbaum constant estimation is reported.
© 2006 Elsevier Ltd. All rights reserved.

Keywords: Bifurcation; Chaos; Plate; Non-homogeneous boundary conditions; Feigenbaum scenario; Bubnov–Galerkin method

1. Introduction

It is well known that non-linear dynamics of plates (shells) plays an important role in both pure and applied sciences as well as in engineering applications. Plates (shells) are members of buildings, bridges, tanks, flight-vehicles, power plants, mechatronical devices, brake systems, etc., and hence a complete knowledge of their dynamic behaviour is highly required [1–4].

The von Kármán equations are used in Ref. [5] to analyse the non-linear vibrations of polar orthotropic clamped plates at elevated temperatures. It has been shown, among others, that thermal stresses reduce the vibrations period. In Ref. [6], the von Kármán equations are used to investigate the non-linear free vibrations of isotropic and polar orthotropic annular plates possessing a rigid mass under action of thermal loads. Finite dimensionality and compactness of attractors for the von Kármán equation are

considered by Lasiecka [7]. More generalized questions are also addressed in Refs. [8–10].

Regular and chaotic vibrations of a plate within von Kármán model are analysed in Ref. [11]. The reduced von Kármán equations are used to study bifurcations of a thin plate-strip excited transversally and axially [12].

The Bubnov–Galerkin approach is applied to analyse both regular and chaotic vibrations together with bifurcations of flexible plate-strips with non-symmetric boundary conditions in Ref. [13]. Some new examples of routes from regular to chaotic dynamics are illustrated and discussed. The phase transitions from chaos to hyper chaos, and a novel phenomenon of a shift from hyper chaos to hyperhyper chaos are outlined.

Flexible plates subjected to longitudinal time constant loading are studied by vast number of researchers. It seems that the most important and fundamental results in this field are reported in Volmir's monograph [14]. From the point of view of qualitative differential equations and non-linear dynamics, the mentioned research subject has been analysed also by the authors in the papers mentioned above and in Ref. [15], but only for classical types of boundary conditions applied to a plate contour. This paper

^{*} Corresponding author. Address: Department of Automatics and Biomechanics, Technical University of Łódź, 1/15 Stefanowskiego St., 90-924 Łódź, Poland. Tel./fax: +48 42 631 22 25.

E-mail addresses: tak@san.ru, awrejcewicz@p.lodz.pl (J. Awrejcewicz).

extends a general approach presented in earlier authors' works for flexible plates with non-homogeneous boundary conditions along their contour.

2. Mathematical model, boundary and initial conditions

The well-known T. von Kármán equations governing dynamics of flexible isotropic plates subjected to a longitudinal load action are analysed in the following form:

$$\frac{\partial^2 w}{\partial t^2} = -\frac{1}{12(1-\nu^2)} \nabla^2 \nabla^2 w + L(w, F) - P_x \frac{\partial^2 w}{\partial x^2} + q, \quad (1)$$

$$\nabla^2 \nabla^2 F = -\frac{1}{2} L(w, w),$$

where q , P_x denote transversal and longitudinal loads, respectively, and ν is the Poisson's coefficient ($\nu = 0.3$).

Boundary conditions applied for the area $\{0 \leq x, y \leq 1\}$ used in this work for $x = 0; 1$ ($x \leftrightarrow y$) read

- (i) simple (ball) support on flexible and unstretched in tangential plane ribs

$$w = \frac{\partial^2 w}{\partial x^2} = F = \frac{\partial^2 F}{\partial x^2} = 0; \quad (2)$$

- (ii) moving clamping with support on flexible and unstretched in tangential plane ribs

$$w = \frac{\partial w}{\partial x} = F = \frac{\partial^2 F}{\partial x^2} = 0. \quad (3)$$

In what follows, various combinations of boundary conditions (2) and (3) not only along the whole plate but also along its one or few sides are considered. A compatibility condition formulated in corners and in points of boundary condition change along the contour side and associated with the boundary conditions (2) and (3) reads

$$\frac{\partial^2 w}{\partial x \partial y} = 0. \quad (4)$$

Initial conditions satisfy the boundary conditions (2) and (3), i.e.,

$$w|_{t=0} = \varphi_1(x, y), \quad \left. \frac{\partial w}{\partial t} \right|_{t=0} = \varphi_2(x, y). \quad (5)$$

In order to choose initial conditions for a case of non-homogeneous boundary conditions, the following approach is applied. The 'set-up' method is used for given boundary condition subjected to an action of small transversal load and the damping $\varepsilon = \varepsilon_{cr}$. The critical value of damping of the surrounding medium corresponds to the forcing value required for achieving a stationary regime through the deflection function within a small time interval. The value of loading q is chosen in a way to keep a deflection value in the plate center less than 10^{-3} . The obtained deflection fields serve as an initial state in order

to investigate non-linear vibrations for the case of non-homogeneous boundary conditions along a contour and an action of the longitudinal load only P_x ($q = 0$).

3. Method of solution

In order to solve dynamical system (1), the algorithm based on combination of finite-difference method and the fourth-order Runge–Kutta method are used. Derivatives with respect to spatial variables are approximated through finite-difference relation of order $O(h^4)$. It allows for reduction of partial differential equations (1)–(5) into the system of linear algebraic equations with respect to the function F (see (7)) and to the system of ordinary differential equations with respect to deflection w (see (6)). The system (7) on each step in time is solved using the upper relaxation method, whereas the system (6) is solved by applying the fourth-order Runge–Kutta method. The difference equations read

$$\frac{d^2 w_{ij}}{dt^2} + \varepsilon \frac{dw_{ij}}{dt} = -\{A_1(w_{ij}) + B_1(w_{ij}, F_{ij})\} + q_{ij}, \quad (6)$$

$$D_1(F_{ij}) = E_1(w_{ij}), \quad (7)$$

and the difference operators have the following form:

$$A_1(w_{ij}) = \frac{1}{12(1-\nu^2)} (\lambda^{-2} L_x^4 w_{ij} + 2L_x^2 L_y^2 w_{ij} + \lambda^2 L_y^4 w_{ij}),$$

$$B_1(w_{ij}, F_{ij}) = L_x^2 w_{ij} (L_y^2 F_{ij} - P_x) + L_y^2 w_{ij} L_x^2 F_{ij} - 2L_x^2 L_y^2 w_{ij} L_x^2 F_{ij}, \quad (8)$$

$$E_1(w_{ij}) = -L_x^2 w_{ij} L_y^2 w_{ij} + [L_{xy} w_{ij}]^2,$$

$$D_1(F_{ij}) = 12(1-\nu^2) A_1(F_{ij}).$$

The difference form of boundary conditions $w = 0$, $\frac{\partial^2 w}{\partial x^2} = 0$ for $x = 1$ and for the out-contour $(i + 1, j)$, $(i + 2, j)$ nodes have the following form:

$$w_{i+1,j} = \frac{1}{11} [-6w_{i-1,j} + 4w_{i-2,j} + w_{i-3,j}],$$

$$w_{i+2,j} = \frac{1}{11} [-80w_{i-1,j} - 75w_{i-2,j} + 16w_{i-3,j}].$$

Analogically, the boundary condition $w = 0$, $\frac{\partial w}{\partial x} = 0$ for $x = 1$ have the following difference form:

$$w_{i+1,j} = \frac{1}{3} [18w_{i-1,j} - 6w_{i-2,j} + w_{i-3,j}],$$

$$w_{i+2,j} = \frac{1}{3} [120w_{i-1,j} - 45w_{i-2,j} + 8w_{i-3,j}].$$

One may formulate boundary conditions for the stress function F . Let us apply the unique form of out of contour nodes in the following form:

$$U_{i+1,j} = \frac{1}{a_1} [a_2 U_{i-1,j} - a_3 U_{i-2,j} + U_{i-3,j}],$$

$$U_{i+2,j} = \frac{1}{a_1} [a_4 U_{i-1,j} + a_5 U_{i-2,j} + a_6 U_{i-3,j}],$$

where the coefficients $a_i (i = \overline{1,6})$ are defined fully with respect to the boundary conditions type. It is worth noticing that the mentioned representation of the boundary conditions allows to solve not only the boundary value problems of types (2) and (3), but also non-homogeneous one, i.e., their combinations along a plate contour. In this case the appropriate compatibility conditions are attached to the system of difference equations. Points where a change of boundary conditions occurs are always located in the mesh nodes.

Recall that, in general, while solving initial boundary value problems of mathematical physics, an important problem associated with a choice of an approximation order of difference scheme occurs. Solving the problems through a difference method one uses a second-order approximation in time of a differential equation and associated initial conditions. It can be increased up to the fourth-order, if one applies the method of straight lines and when the fourth-order Runge–Kutta method is used to solve the differential difference equations. In the latter case, an initial condition ($\partial w / \partial t = \varphi_2(x, y)$) is given in exact manner. Since an approximation with respect to spatial coordinates x and y is of order $O(|h|^4)$, larger mesh can be used in order to achieve the required accuracy.

The last factor allows to decrease essentially the order of the system of differential difference equations, which is very important during solving multidimensional problems. This remark stays in agreement with hyperbolic type equations, i.e., equations governing dynamics of strings, membranes and plates. Investigations have been carried out for various model problems. As a result, the following main conclusion has been achieved: the most optimal method is that of straight lines (with an application of approximation with respect to spatial coordinates $O(|h|^4)$) matched with the fourth-order Runge–Kutta method.

On the other hand, while solving a system of linear difference equations of a high order with a matrix possessing large zero elements, a problem of an appropriate algorithm choice appears.

Notice that one is going to choose the method characterized by a minimal time of solutions of the stated problem in comparison with other ones. In order to achieve an optimal choice of the algorithms they are compared due to the number $Q(\varepsilon_0)$ of arithmetical actions required to find solutions of the considered problems with a priori given accuracy.

Our numerical tests show that in order to solve a system of high order difference equations, the most efficient method is the upper relaxation method. It is more economical and effective than the Gauss method, at least in the case of our investigated plate.

The choice of h in respect to spatial coordinates and a step in time τ in the Runge–Kutta method is realized through the Runge principle. The experiments carried out yield the step $h = 1/8$ and $\tau = 0.00025$ owing to the fact that for time step $\tau = 0.00025$, the values of the stress functions obtained on a previous time step serve as a good initial approximation for the next computational layer.

The iterational parameter ω can be practically equal to one, i.e., Seidel method can be applied.

The reliability of the results is verified through the comparison with solutions of the series of non-linear problems of theory of plates achieved by other authors, with solutions of test and modal problems and through checking convergence in relation to the number of mesh points used for spatial coordinates. The comparison of the results obtained through finite-difference methods approximations of order $O(h^4)$ and $O(h^2)$ is carried out. Reliability of the results in dynamical problem with non-homogeneous boundary conditions along a contour is verified through a good agreement of solutions obtained due to ‘set-up’ method and due to static methods for the same boundary conditions applied.

4. Results

In what follows, eight types of different boundary value problems (denoted 1–8) are studied.

Problem 1. Part of the contour $\{0 \leq x \leq 0.5; y = 1\}$ satisfies condition (3), whereas the remaining contour part satisfies condition (2). *Problem 2.* One square side of the plate, i.e., $\{0 \leq x \leq 1; y = 1\}$ satisfies condition (4), whereas the other parts satisfy condition (2). *Problem 3.* Part of the boundary, namely $\{0 \leq x \leq 1; y = 1\} \{x = 1; 0.5 \leq y \leq 1\}$ satisfies condition (3), whereas the remaining contour part satisfies condition (2). *Problem 4.* Two square sides, namely $\{0 \leq x \leq 1; y = 1\} \{x = 1; 0 \leq y \leq 1\}$ satisfy condition (3), and the remaining contour part satisfies condition (2). *Problem 5.* Part of the contour, i.e., $\{0 \leq x \leq 1; y = 1\} \{x = 1; 0 \leq y \leq 1\} \{0.5 \leq x \leq 1; y = 0\}$ satisfies condition (3), and the rest of the contour satisfies condition (2). *Problem 6.* Three sides of the square, i.e., $\{0 \leq x \leq 1; y = 1\} \{x = 1; 0 \leq y \leq 1\} \{0 \leq x \leq 1; y = 0\}$ satisfy condition (3), and the remaining contour part satisfies condition (2). *Problem 7.* Part of the boundary, i.e., $\{x = 0; 0.5 \leq y \leq 1\}$ satisfies condition (2), and the remaining contour part satisfies condition (3). *Problem 8.* Boundary conditions (3) are satisfied along the whole contour plate.

Our main research interest is focused on various scenarios of the investigations of vibrations of square plates made from an isotropic material with non-homogeneous boundary conditions subjected to an action of longitudinal impact pulse $P_x = P_k = \text{const}$. The damping coefficient $\varepsilon = 0$ is taken in the system we consider (1), i.e., we analyse a conservative problem. It is worth noticing that for all eight problems considered, the scenario characterizing transition into dynamical instability is practically the same.

Recall that in 1978 Feigenbaum detected the universal constant value responsible for transition to chaos through a sequence of period doubling bifurcations associated with one dimensional maps of the form $x_{n+1} = f(x_n, P_0)$. A class of the considered functions should be smooth and non-singular, and $f(x)$ should be approximated through quadratic terms in vicinity of its maximum. The mentioned maps are parabolic, and they describe unique (but not self-unique)

transformations into itself. Observe that in our investigations we have not used the mapping $x_{n+1} = f(x_n, P_0)$, but the Feigenbaum constant has been found numerically. To achieve this goal, the following algorithm has been applied: (1) initial conditions of the analysed problem are defined through the ‘set-up’ method; (2) period of free vibrations T_0 is found numerically; (3) a sequence of $\{P_k\}$ associated with the occurrence of period doubling bifurcations $\{T_0, 2T_0, 4T_0, 8T_0, \dots\}$ is obtained numerically.

It is clear that while increasing k , the ratio $(P_{k+1} - P_k) / (P_{k+2} - P_{k+1})$ should tend to the constant value of $\delta = 4.669201\dots$. Analysis of the obtained results yields a conclusion that for all analysed cases $\delta \approx 4.66$.

In order to carefully analyse transitions from quasi-periodic to chaotic vibrations, as well as to analyse various mechanisms of transition between system dynamical states we have applied different vibration characteristics like phase and modal portraits, Fast Fourier Transform

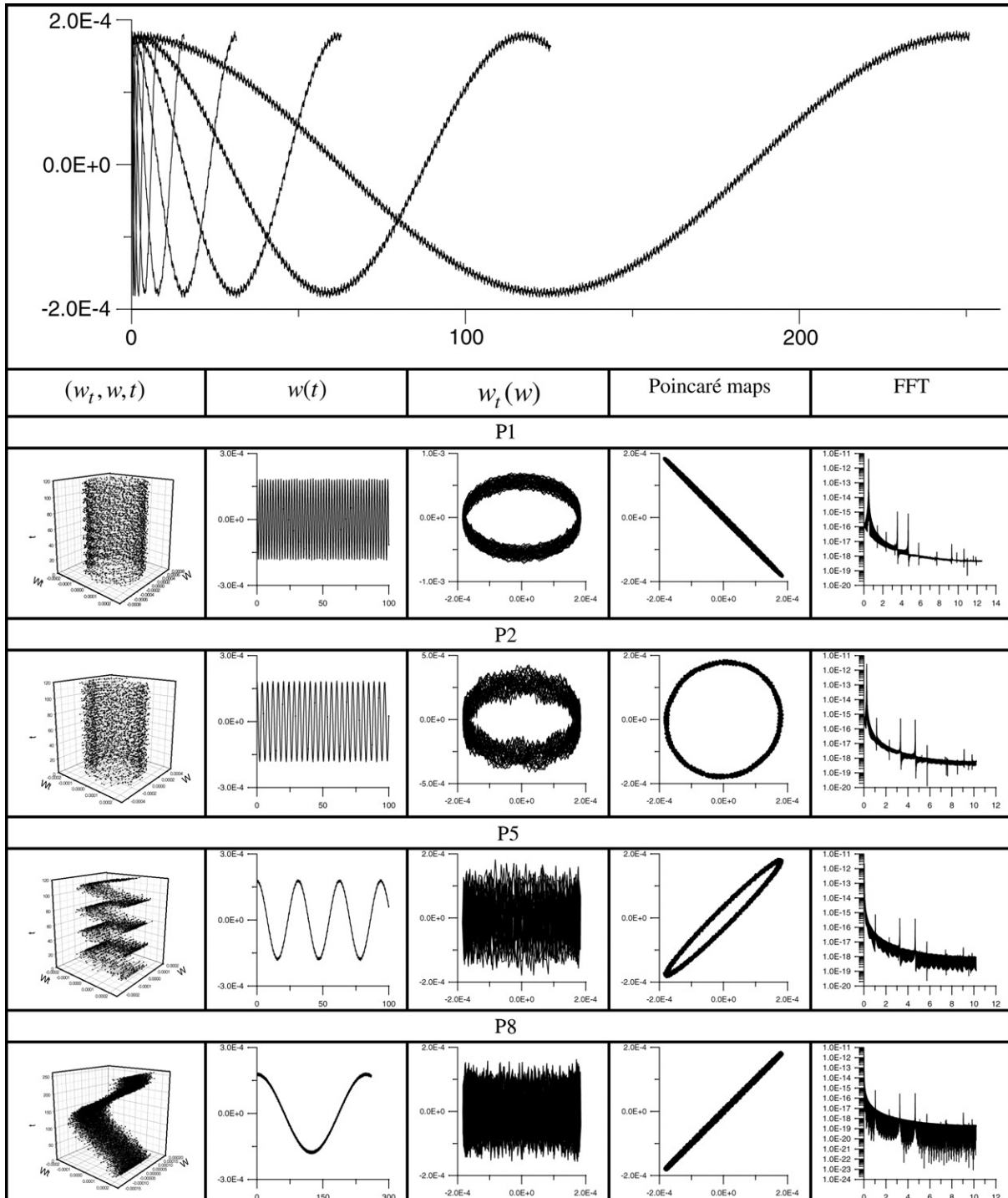


Fig. 1. Computational results associated with Problem 1.

(FFT), power spectra, and Poincaré maps. In Figs. 1–3 some of the mentioned characteristics are reported for Problems 1, 5 and 6, as well as time histories $w(t)$ for the values of P_k for which period doubling bifurcations occur.

Our investigations show that an increase of P_k causes an occurrence of a broadband frequency spectrum. Amplitudes of this ‘noisy’ frequency spectrum essentially depend on the applied boundary conditions (Figs. 2 and 3). If instead of three-dimensional phase portrait one considers its projection onto the plane $w_t(w)$, then a broadband characteristic is obtained. This can be also interpreted as noisy chaos with respect to both frequency spectrum and phase portrait projection into a plane.

Among others, the essential influence of the boundary conditions on the amount of bifurcations has been detected (Table 1). For instance, Problems 1–5, 7 are associated with eight bifurcations, Problem 6 is associated with seven period doubling bifurcations, whereas Problem 8 corresponds to nine period doubling bifurcations. It should be emphasized that a percentage of the plate contour clamping from an interval of 62.5–100% essentially influences the number of bifurcations as well as the character of the amplitude ‘noisy’ components.

Observe that an increase of P_k on amount of 1×10^{-4} just after achieving of P_k^* yields the first ‘stiff’ stability loss. Namely, a change of vibrations form, phase portrait, period of vibrations, as well as the increase of vibrational amplitude of an order amount are observed. The behaviour described so far occurs on a very small interval of P_k variation.

Further increase of the parameter P_k forces the system to exhibit a stiff stability loss with a deflection increase in amount of 10^3 times (Fig. 4 contains results associated with Problem 1). This means that the system jumps into another equilibrium state. New vibrations that occur possess large amplitude and take place around a new equilibrium position. A typical chaotic interlacing of the curves in the phase portrait is observed, Poincaré pseudo-maps are characterized by a chaotic points distribution, whereas one may also observe a broadband threshold on the FFT diagram. The latter observations can be associated with the so-called final chaotic state of the analysed system.

The systems of Eqs. (1) can be cast into the following form:

$$\frac{d^2 w}{dt^2} + L_1(w) = 0, \tag{9}$$

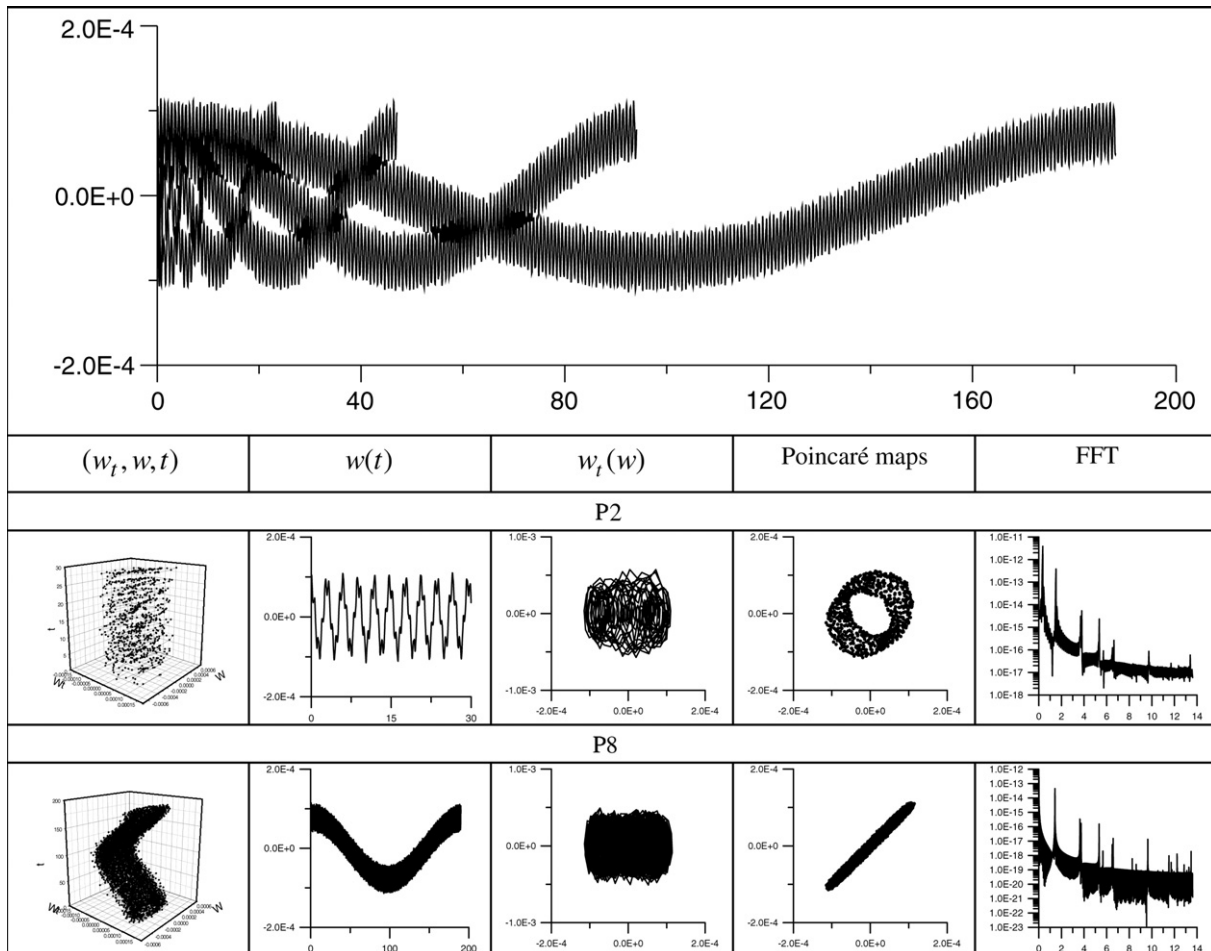


Fig. 2. Computational results associated with Problem 5.

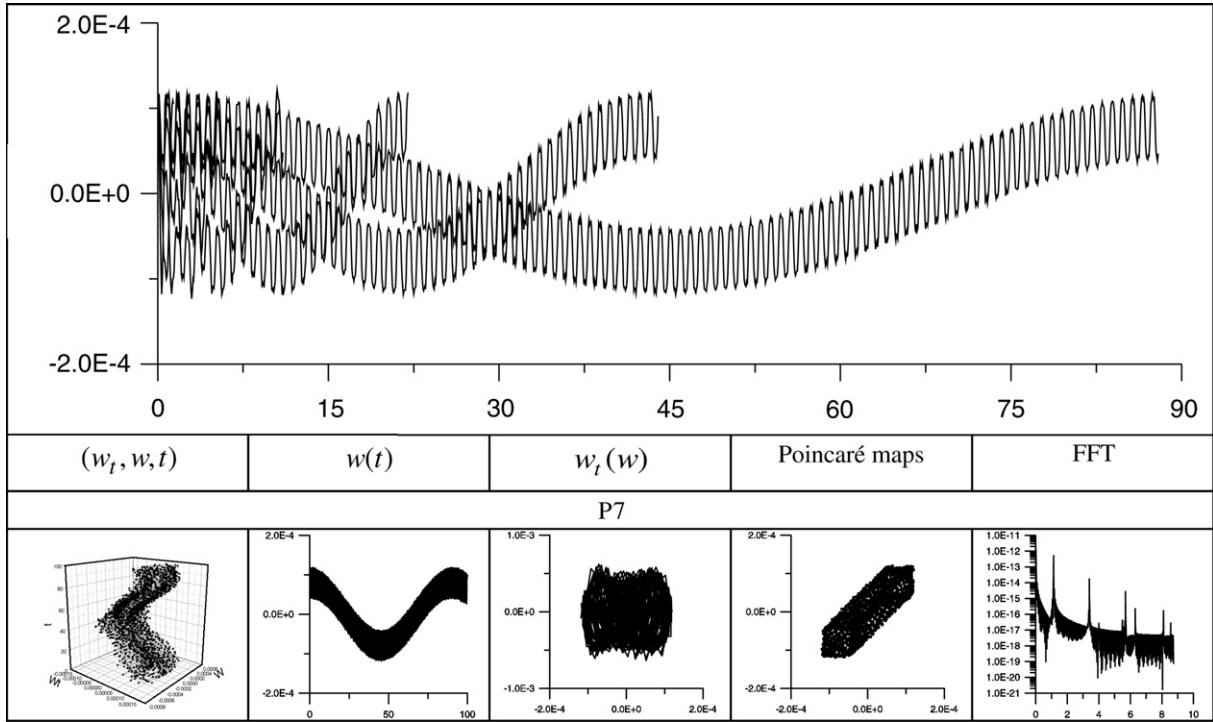


Fig. 3. Computational results associated with Problem 6.

Table 1
Number of bifurcations versus contour clamping type

Problem number	Contour clamping (%)	Bifurcation number
1	12.5	8
2	25	8
3	37.5	8
4	50	8
5	62.5	8
6	75	7
7	87.5	8
8	100	9

where $L_1(w)$ is a non-linear differential operator associated with spatial coordinates (x, y) . Assume that a solution w_t to Eq. (9) is found with a help of one of the existing methods. Consider now a small perturbation δw of the solution w_t in time instant t . Then one may write

$$w = w_t + \delta w, \tag{10}$$

which satisfies Eq. (9). Substituting (10) into (9), one gets

$$\frac{d^2 \delta w}{dt^2} + L(w_t + \delta w) - L_1(w_t) = 0. \tag{11}$$

Notice that Eq. (11) is a non-linear one with respect to perturbations, and its variable coefficients w_t are defined through a solution carried out for each point of the initial equation (9). Owing to small perturbations in Eq. (11), one may retain only linear terms, i.e., finally the following second-order differential equation is analysed:

$$\frac{d^2 \delta w}{dt^2} + \omega^2 \delta w = 0. \tag{12}$$

Its solution follows:

$$\delta w(t) = H \cos(t\omega + \varphi) \quad \text{if } \omega^2 > 0, \tag{13}$$

$$\delta w(t) = Ht + R \quad \text{if } \omega^2 = 0, \tag{14}$$

$$\delta w(t) = He^{t\sqrt{-\omega^2}} + Re^{t\sqrt{-\omega^2}} \quad \text{if } \omega^2 < 0, \tag{15}$$

where H and R are the integration constants.

5. Concluding remarks

With the above formulas, one may conclude that if all $\omega^2 > 0$, then the solution is stable, and the associated perturbation is a combination of two harmonic components with the frequency ω . In all other cases the solution is unstable, i.e., perturbations increase in an exponential manner. The latter observation leads to the following conclusion: having a spectrum of small perturbations in each point of the analysed system, one may decide on stability or instability of solution in three points.

It is obvious that in the instant of stiff stability loss the small perturbations, which are clearly visible in our numerical experiment, possess imaginary parts of squared frequencies, and hence they are responsible for dynamical stability loss of the system.

The variation of P_x on amount of 1×10^{-4} causes a stiff stability loss of our system. The existence of chaotic vibrations is also observed here. Birth and death of some sequences of cycles are observed, as well as series of Andronov–Hopf bifurcations appear. Time interval associated

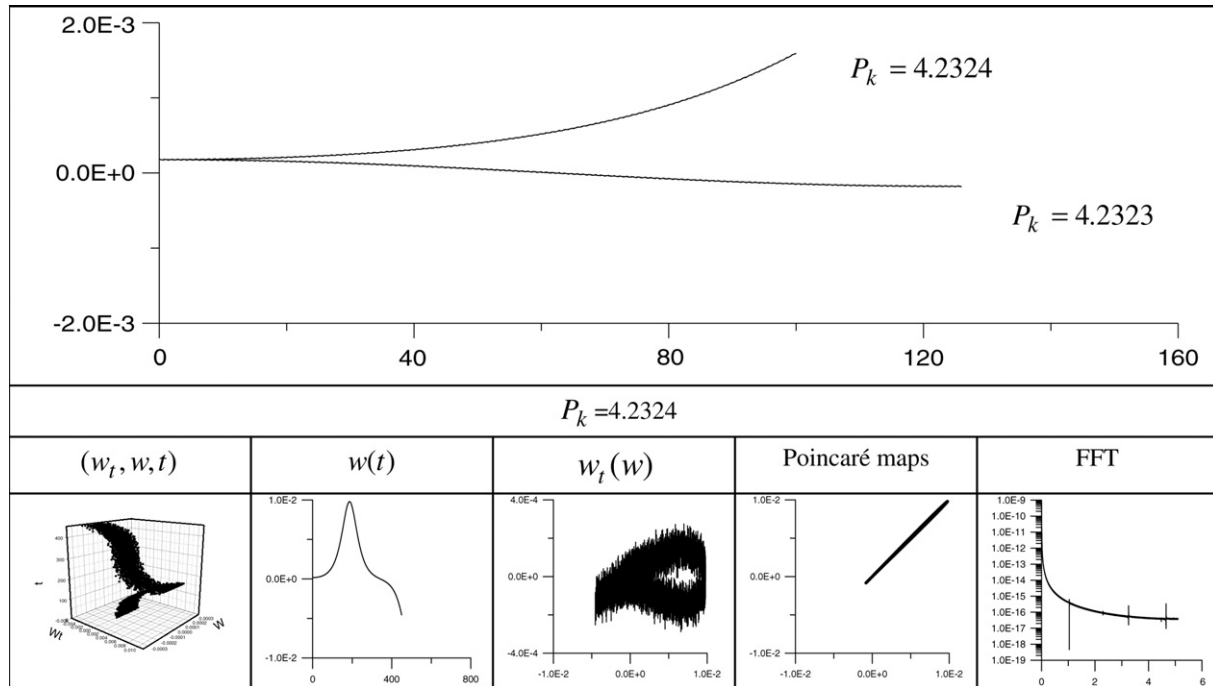


Fig. 4. Computational results associated with Problem 1 ($P_k = 4.2324$).

with the occurrence of stiff stability loss is the largest one in this case, i.e., while changing slowly the parameter P_x , a stiff stability loss is observed. On the other hand, time interval required for achieving stability loss decreases with the increase of P_x .

Furthermore, one may find threshold of P_x when stability loss occurs in practice suddenly, and the so-called final chaotic state is observed.

On the other hand, one may conclude that even for P_x^{cr} corresponding to time interval t_{cr} , if a researcher is interested in time interval ($t \leq t_{cr}$), a dynamical stability loss is not important for the considered time interval. In other words, unrequired large perturbations of the fundamental motion can appear only after $t > t_{cr}$. Furthermore, controlling the series of Andronov–Hopf bifurcations, one may avoid an occurrence of stiff stability loss.

References

- [1] Bolotin VV. The dynamic stability of elastic systems. San Francisco: Holden-Day; 1964.
- [2] Ciarlet PG. Mathematical elasticity. Theory of plates, vol. 2. Amsterdam: Elsevier; 1997.
- [3] Dowell EH. Aeroelasticity of plates and shells. Leiden: Nordhoff; 1974.
- [4] Volmir AS. Nonlinear dynamics of plates and shells. Moscow: Nauka; 1972 [in Russian].
- [5] Biswas P, Kapoor P. Non-linear vibrations of circular plates at elevated temperature. In: Proceedings of fourth int conf on numerical methods in thermal problems, Part 2, Swansea, UK, July 15–18, 1985. p. 1493–501.
- [6] Li S-R, Zhou Y-H, Song X. Non-linear vibration and thermal buckling of an orthotropic annular plate with a centric rigid mass. J Sound Vibr 2002;251:141–52.
- [7] Lasička I. Finite dimensionality and compactness of attractors for von Kármán equations with nonlinear dissipation. Nonlinear Differen Equat Appl 1999;6:437–72.
- [8] Krysko VA, Awrejcewicz J, Bruk V. On the solution of a coupled thermo-mechanical problem for non-homogeneous Timoshenko-type shells. J Math Anal Appl 2002;273(2):409–16.
- [9] Krysko VA, Awrejcewicz J, Bruk V. On existence and uniqueness of solution to coupled thermomechanics problem of non-homogenous isotropic plates. J Appl Anal 2002;8(1):129–39.
- [10] Awrejcewicz J, Krysko VA. Nonclassical thermoelastic problems in nonlinear dynamics of shells. Berlin: Springer; 2002.
- [11] Awrejcewicz J, Krysko VA, Krysko AV. Spatio-temporal chaos and solitons exhibited by von Kármán model. Int J Bifurc Chaos 2002;12(7):1465–513.
- [12] Awrejcewicz J, Krysko VA, Narkaitis GG. Bifurcations of a thin plate-strip excited transversally and axially. Nonlinear Dynam 2003;32:187–209.
- [13] Krysko VA, Awrejcewicz J, Narkaitis GG. Nonlinear vibration and characteristics of flexible plate-strips with non-symmetric boundary conditions. Commun Nonlinear Sci Numer Simul 2006;11(1):95–124.
- [14] Volmir AS. Stability of elastic systems. Moscow: Science; 1972.
- [15] Awrejcewicz J, Krysko VA. Feigenbaum scenario exhibited by thin plate dynamics. Nonlinear Dynam 2001;24:373–98.